Supporting Information

High-Performance Asymmetric Supercapacitor Device with Trimetallic Sites Encapsulated in Multilayered Nanotube

Rahul Patil[a #]; Lingaraj Pradhan,[b,c #]; Babasaheb Matsagar[d]; Omnarayan Agrawal[a]; Kevin Chia-Wen Wu[d,e,f]; Bikash Kumar Jena[b,c]; Saikat Dutta[a]**

[a]Electrochemical Energy & Sensor Research Laboratory, Amity Institute of Click Chemistry Research & Studies, Amity University Noida, India
sdutta2@amity.edu
[b]CSIR-Institute of Minerals and Materials Technology, Bhubaneswar-751013, India

[c]Academy of Scientific and Innovative Research (AcSIR), Ghaziabad 201002, India

bikash@immt.res.in

[d]Department of Chemical Engineering, National Taiwan University, No. 1, Sec. 4, Roosevelt Road, Taipei 10617, Taiwan

[e]Department of Chemical Engineering and Materials Science, Yuan Ze University, Chung-Li, Taoyuan, Taiwan

#Both the authors contributed equally.

S1. Materials and Instrumentation.

All chemicals were purchased from commercial sources and used without further treatment: zinc nitrate hexahydrate ($Zn(NO_3)_2 \cdot 6H_2O$, Sigma Aldrich, 99%), 2-methylimidazole (Sigma-

Aldrich, 99%), cobalt nitrate hexahydrate (Sigma-Aldrich, 99%), nickel nitrate hexahydrate(Sigma-Aldrich, 99%).

S2. Experimental

Synthesis of Tri-metallic ZIF (M-ZIF)

Tri-metallic ZIF was synthesized via solvothermal method as per previous reported method with modified Co ratio.[1] Typically, $Zn(NO_3)_2.6H_2O$ (0.8961; 1mmol), $Co(NO_3)_2.6H_2O$ (1.754; 2mmol), $Ni(OAc)_2.4H_2O$ (1.4955;2mmol), in 45ml methanol and mixed together using magnetic stirrer till 45 minutes. This mixture was sonicated for 20 mins. After that 2-methylimidazole (6.8934; 28mmol) was transferred to the trimetallic mixture with continuous stirring. This reaction mixture was transferred to the in 50 ml Teflon °vessels and heat it at 90°C for 21 hrs. The mixture was collected and then Centrifuge the mixture at 8000 rpm for 10 mins. Resuspend the pellet in absolute water and ethanol and centrifuge it at 8000 rpm for 5mins. Repeat this step twice. After that sample was dried at 60 ^{o}C for 12 hours in vacuum oven to prevent the oxidation of metallic sites.

M-ZIF Carbonization to obtain C-ZIF-800

Typically, the ground Tri-metallic ZIF was homogeneously dispersed in a ceramic boat before placing the ceramic into a tube furnace. After the sample was exposed to a flow of argon at room temperature for 30 min, the furnace was heated to the (targeted carbonization temperature) 800 °C for 8 hour with a heating rate of 5 °C/min. Then, the resulting sample was extensively washed using a 2M concentration of H_2SO_4 to remove unstable metallic species. Next, the sample was washed several times with deionized water and absolute ethanol before drying in an vaccum oven at 60 °C for 12 hours.

Preparation of C-ZIF-700

For comparison, C-ZIF-700 prepared as per privously reported method and ratio [1].

Electrochemical measurements

The electrochemical performance, such as cyclic voltammograms (CV), galvanostatic charge-discharge (GCD), and electrochemical impedance spectroscopy (EIS) measurements was examined in a three-electrode system taking 1 M KOH as electrolyte. All the electrochemical experiments are performed by a Bio-logic instrument (EC. Lab, V: 10.37), taking the Ag/AgCl (Sat. KCl) and bare platinum wire as the reference and auxiliary electrode and the sample modified glassy carbon electrode (GCE, geometrical surface area 0.07 cm^2) as the working electrode. Before the electrochemical measurements, the GCE was polished by alumina slurry (of sizes 1μ, 0.3μ, and 0.05μ sequentially), followed by bath sonication against deionized water and vacuum dried.

To get the specific capacitance from the CV curves, we used the following formulas:

$$C_{sp} = \frac{1}{\mathrm{v}.\Delta\mathrm{V}.\mathrm{m}} \int i(V)dV \qquad (1)$$

Here C_s is the specific capacitance (F g^{-1}), v is the scan rate (V s^{-1}), ΔV is the voltage range (V), m is the mass of materials, and I is the positive current of the CV curve (Equation 1). For the asymmetric supercapacitors of the two-electrode system, specific capacitance obtained from GCD curves was calculated using the following equations:

$$C_{sp} = \frac{I_m \Delta t}{\Delta\mathrm{V} - \mathrm{IR}} \qquad (2)$$

Specific capacity (Qs) = Cs × ΔV (3)

Here, I_m is the discharge current density (A g^{-1}), V is cell voltage after iR drop, and Δt is the discharge time (s) and Qs is the Specific capacity (mAh $g^{-1,}$ or C g^{-1}).

The specific energy (E, W h kg^{-1}) and specific power (P, W kg^{-1}) densities were calculated from GCD curves as follows:

$$E = \frac{C_s V^2}{7.2} \quad (3)$$

$$P = \frac{E*3600}{t} \quad (4)$$

Here "t" is the discharge time of the supercapacitor in seconds.

The reaction kinetics can be explained by Dunn's method, which gives information about diffusion-controlled processes. The current calculated from this method is

$$I(\nu) = k_1 (\nu)^{0.5} + k_2 \nu \quad (5)$$

$$\frac{I(\nu)}{\nu^{0.5}} = k_1 + k_2 \nu^{0.5} \quad (6)$$

Where k_1, k_2, and ν are intercept, slope, and scan rate for C-ZIF-800 at different scan rates.

The cathode and anode charges can be balanced using mass balance for optimum electrochemical outcomes in hybrid asymmetric supercapacitors.

The cathode and anode charges can be balanced using mass balance for optimum electrochemical outcomes in hybrid asymmetric supercapacitors.

$$\frac{m+}{m-} = \frac{Cs-\Delta V-}{Cs+\Delta V+} \quad (7)$$

Where m (+ or -), V (+ or -), and C (+ or -) are mass (g), voltage (V), and specific capacitance (F g^{-1}) of positive and negative electrodes, respectively.

Characterizations

X-ray photoelectron spectroscopy (XPS) measurements were performed by using XPS - NEXSA ThermoFisher Scientific with Al K-alpha source (hν = 1486.6 eV) as the excitation source. Field-emission scanning electron microscopy (FE-SEM) was carried out with a

FESEM- JEOL 7900F (at an acceleration voltage of 5 kV). Powder X-ray diffraction patterns (PXRD) were collected on a Japan Rigaku Mini flex 600 rotation anode X-ray diffractometer equipped with graphite monochromatized Cu Kα radiation (λ = 1.54 Å). The transmission electron microscopy (TEM), high-resolution TEM (HRTEM) and high-angle annular dark-field scanning transmission electron microscopy (HAADF-STEM) images were acquired on JEOL-2010 instrument. The aberration-corrected HAADF-STEM measurements were taken on a JEM-ARM200F instrument at 200 keV. The nitrogen and carbon dioxide sorption isotherms were measured by using the automatic volumetric adsorption equipment (Micromeritics ASAP 2020). Prior to gas adsorption/desorption measurement, the samples were dried for 12 h at 433 K under vacuum. The X-ray absorption fine structure (XAFS) spectra (Ni K-edge) were recorded at the Beam line 09, RRCAT Indore Madhya Pradesh India. The electron storage ring of NSRRC was operated at 1.5 GeV with a current of 300 mA. Using Si (111) double-crystal monochromator, the data collections were carried out in transmission mode using ionization chamber for Ni foil and NiO, and in fluorescence excitation mode using a Lytle type detector for ZIF-8 and C-ZIF-800. All measurements were made at room temperature with solid samples.

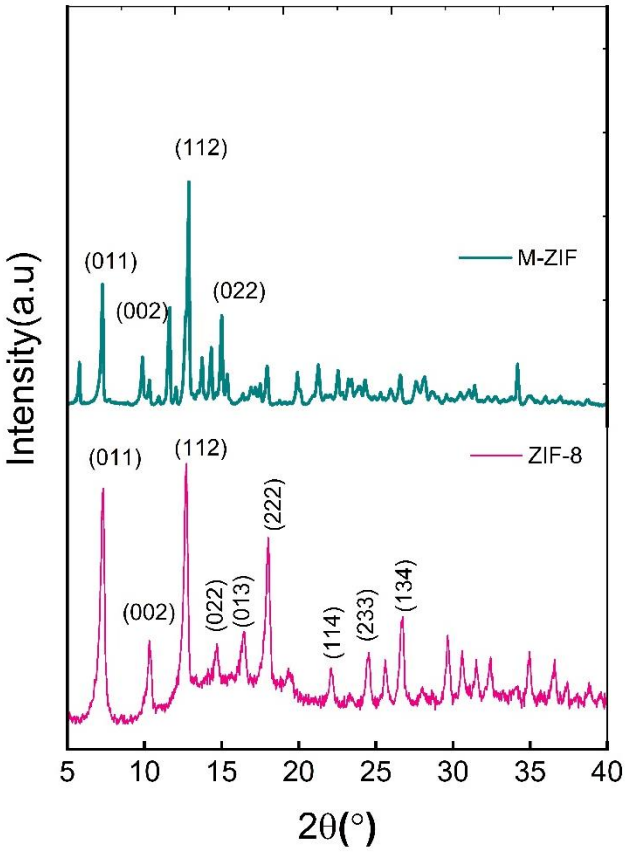

Figure S1. XRD of M-ZIF compared with ZIF-8.

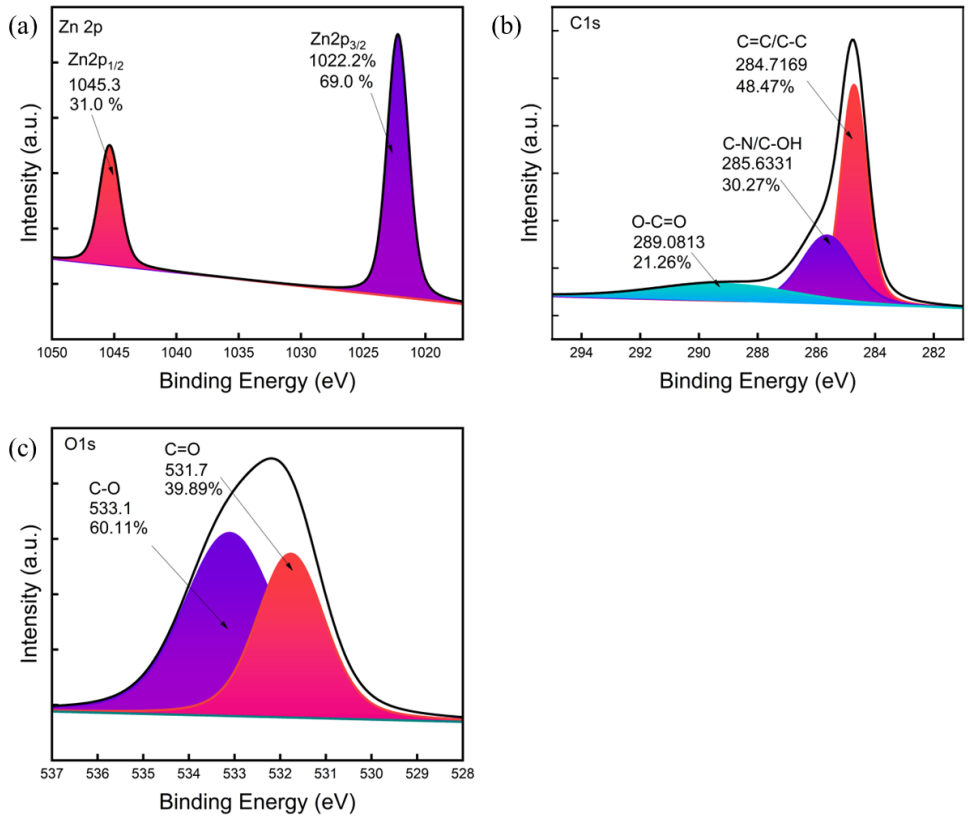

Figure S2. XPS deconvoluted plot of (a) Zn2p (b) C1S and (c) O1s of C-ZIF-800.

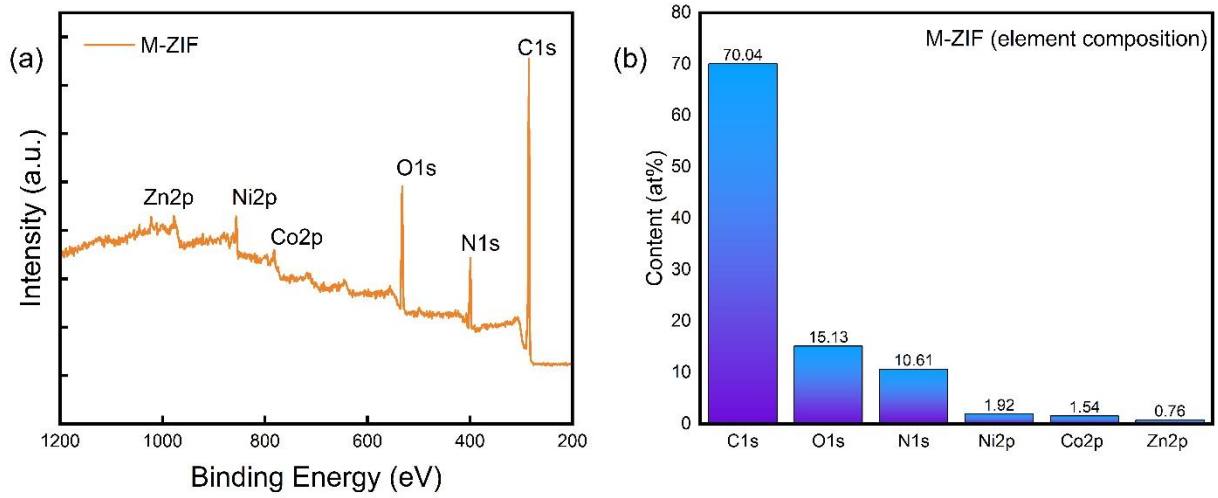

Figure S3. (a) Survey spectra of M-ZIF and (b) Elemental content of M-ZIF, obtained from XPS.

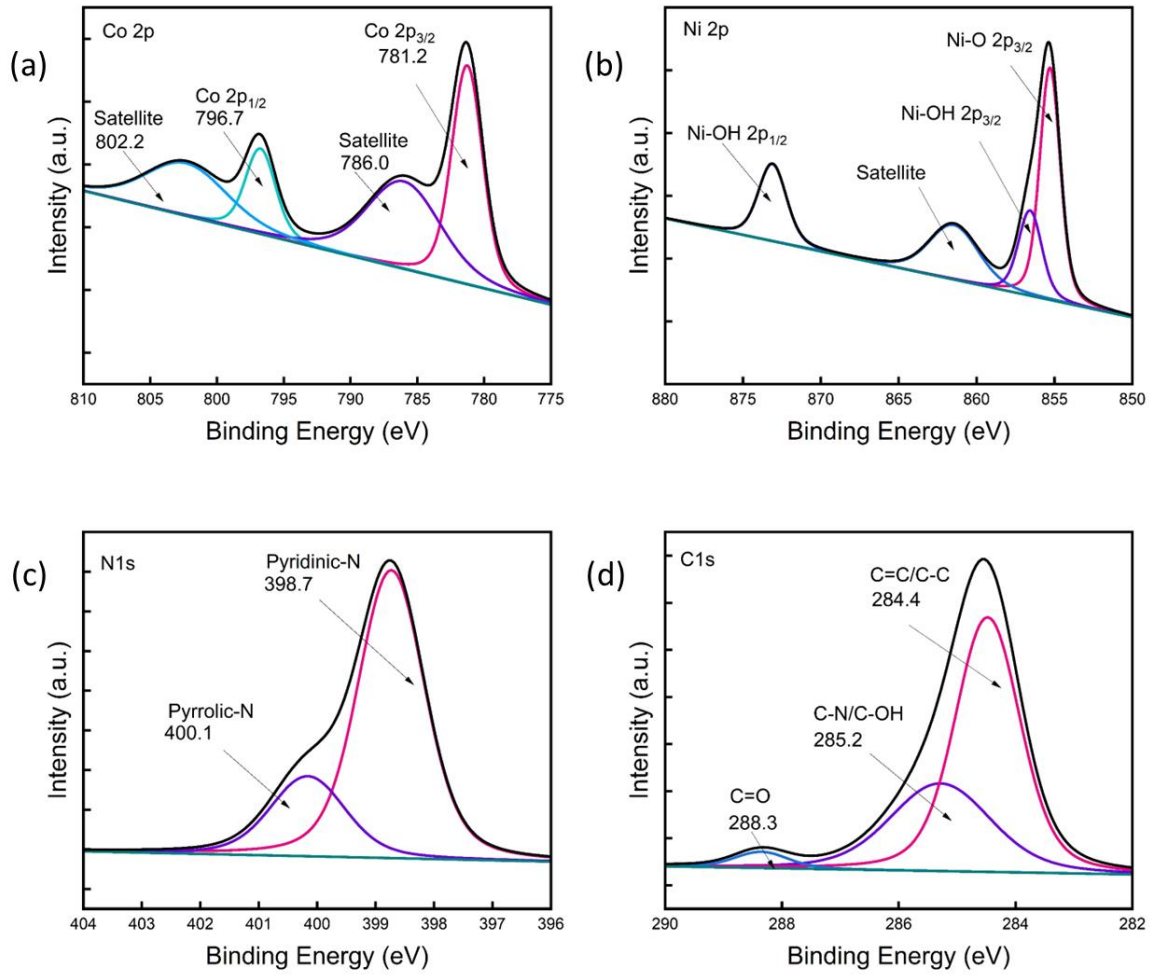

Figure S4. XPS deconvoluted plot of (a) Co 2p (b) Ni 2p (c) N1s and C1s of M-ZIF

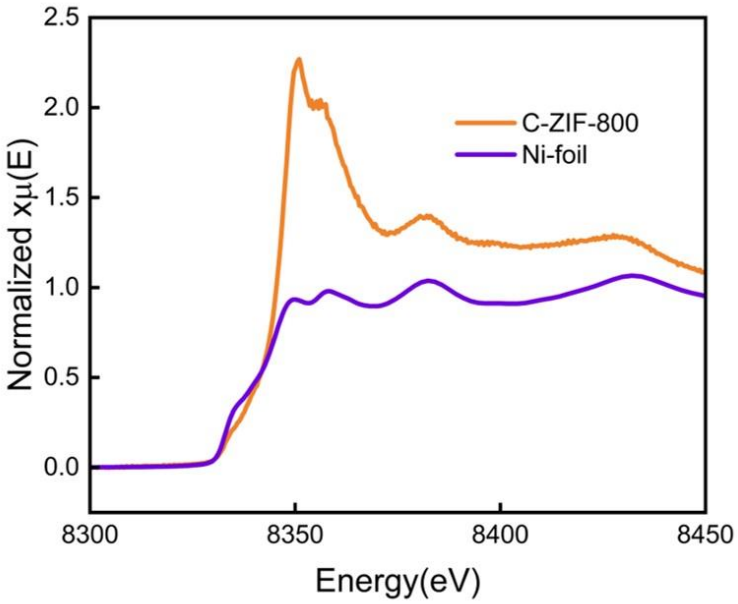

Figure S5. XAS spectra of C-ZIF-800 contains relative intensities and edge positions.

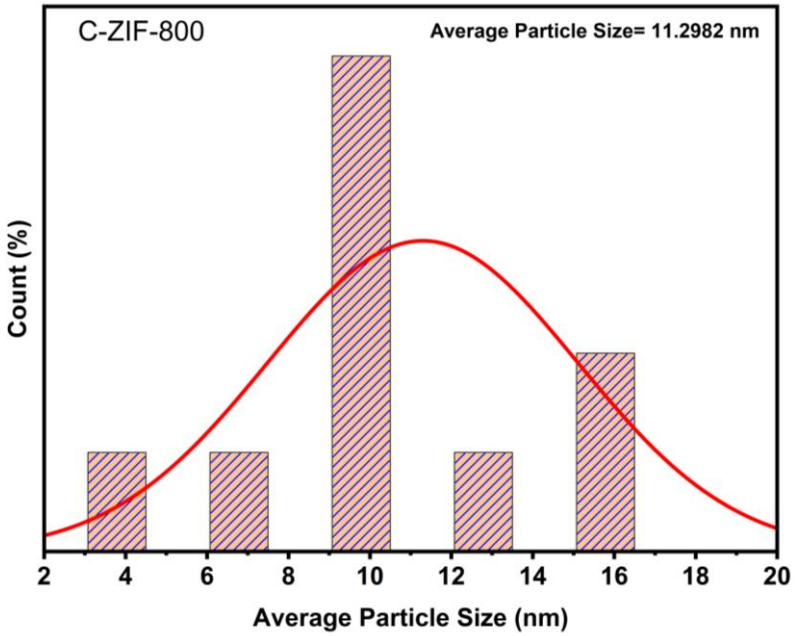

Figure S6 The average particle size of metal centers in C-ZIF-800 calculated from TEM.

Moreover, the average $Crystallite\ size$ was found 5.80 nm for C-ZIF-800 sample.

The crystallite size of C-ZIF-800 was calculated from the Scherrer's formula,

$$Crystallite\ size(D) = \frac{K\lambda}{\beta\cos\theta} \qquad (8)$$

where θ indicate the angle between the incident and reflected X-rays, β is the full width at half maxima, λ is the X-ray wavelength = 1.5406 Å (Cu Kα), and K is the shape factor constant = 0.89.

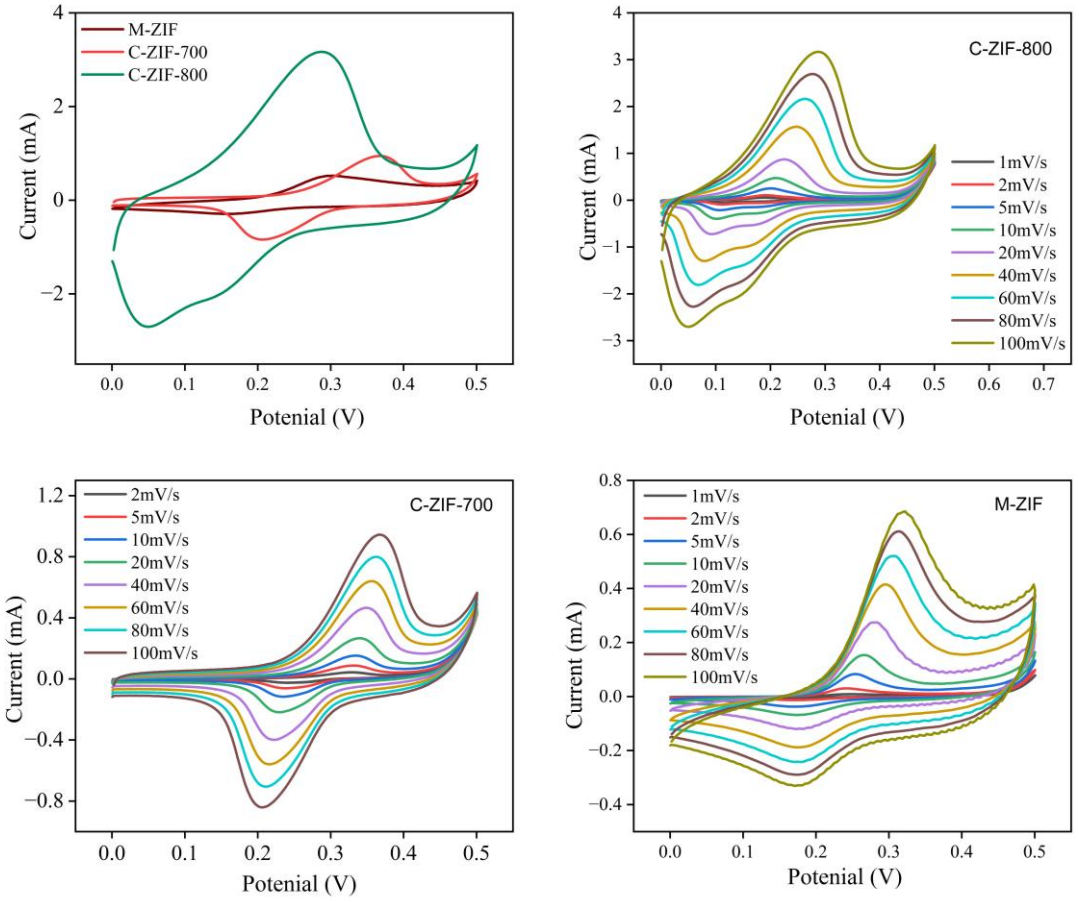

Figure S7. (a) CV profile by varying the synthesis temperature CV plot at different scan rate from 1 to 100 mV.s^{-1} for **(b)** C-ZIF-800, **(c)** C-ZIF-700**, (d)** M-ZIF.

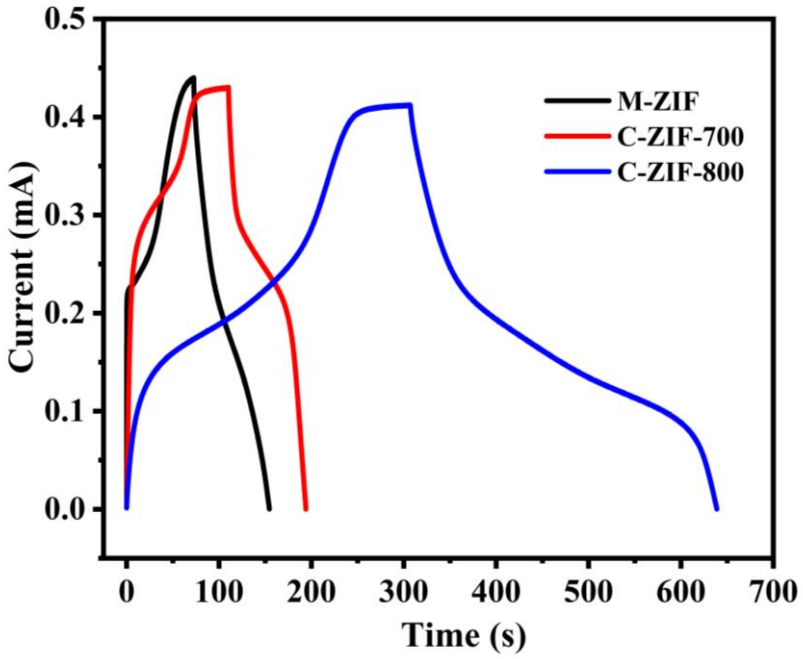

Figure S8. GCD profile by varying the synthesis temperature at 1 A/g.

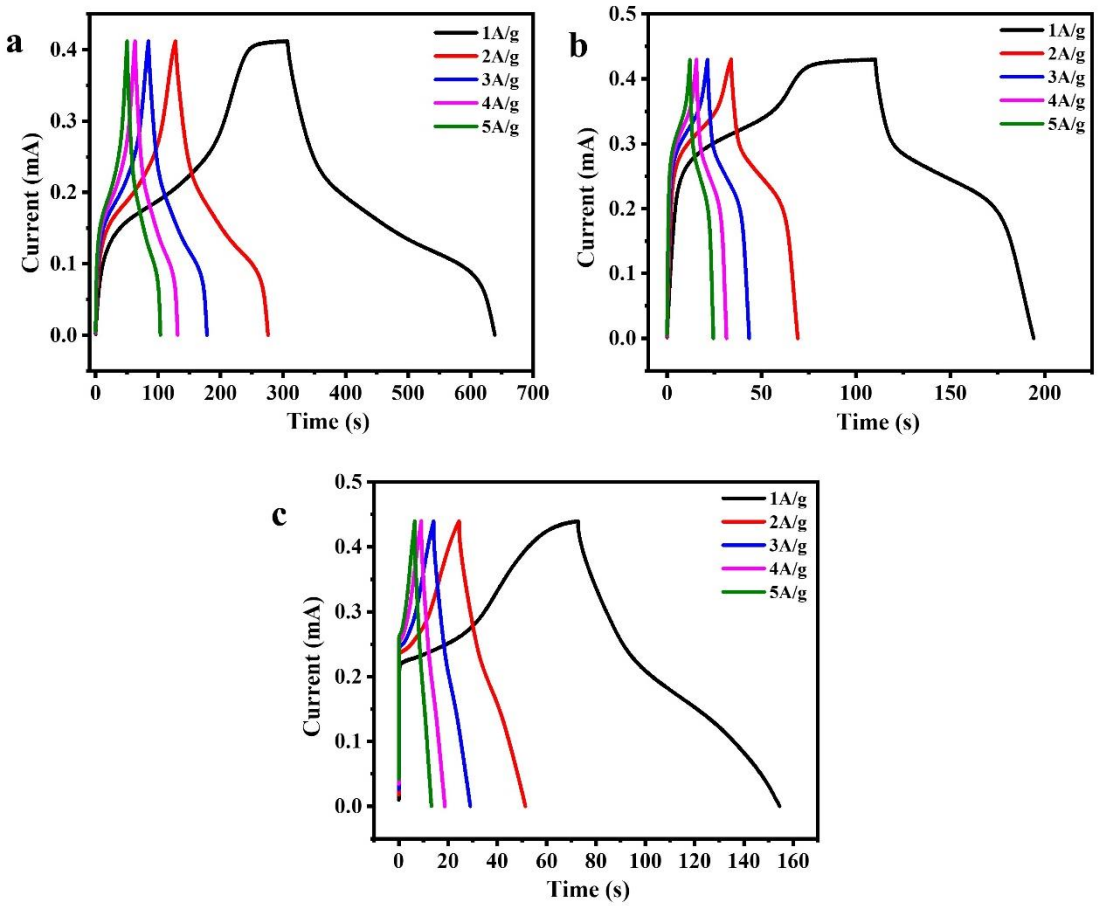

Figure S9. GCD plot at different current densities from 1 to 5 $A.g^{-1}$ for (a) C-ZIF800, (b) C-ZIF700, (c) M-ZIF.

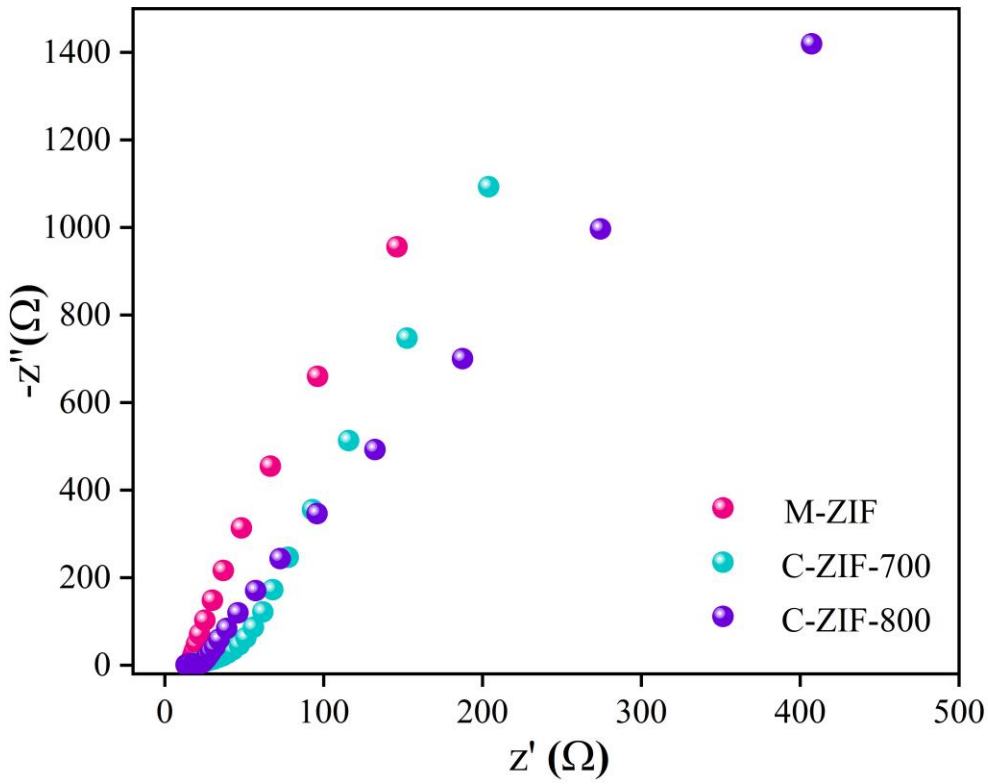

Figure S10. Electrochemical Impedance Spectroscopy (EIS) plot of all the variations.

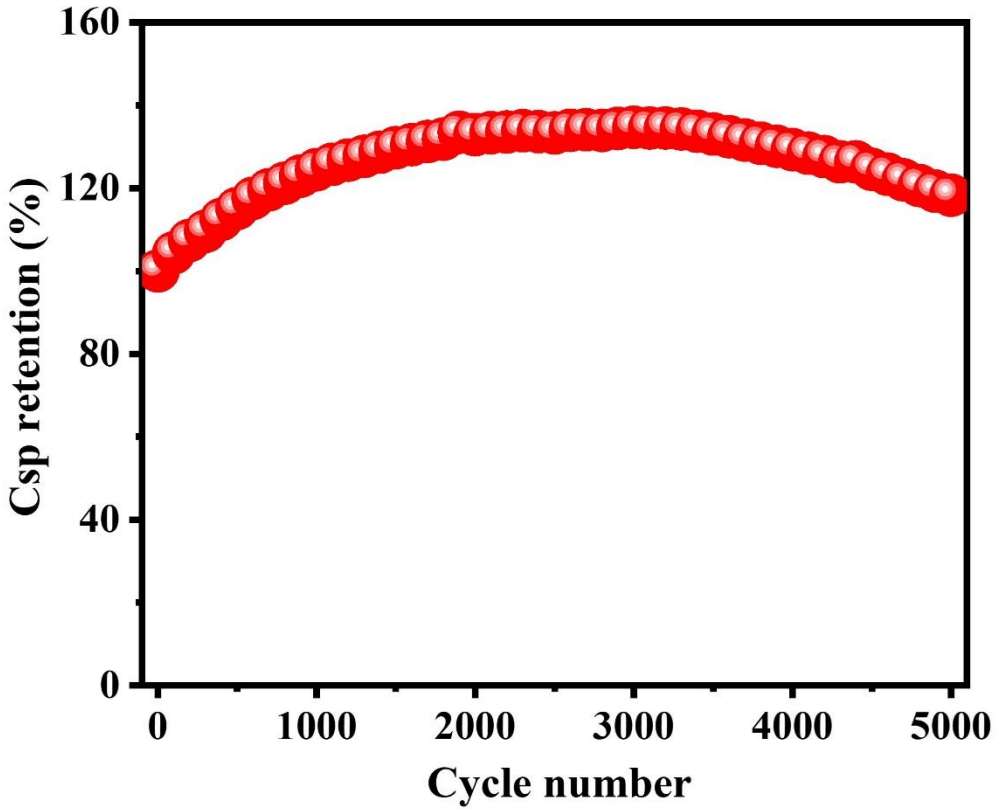

Figure S11 Cycle stability test for 5000 cycles in 3 electrodes measurements.

Table S1. Asymmetric device performance of C-ZIF-800 with similar materials.

Entry	Materials	Electrolyte	Energy density (Wh/kg^{-1})	Power density (W/kg^{-1})	Capacitance retention (%)/Cycle number	Ref.
1	CH@Ni-MOFs	6M KOH	29.9	800	90.1%/10 000	[2]
2	Try-Ni-MOF	3M KOH	66.55	349	92.12%/5 000 cycles)	[3]
3	Ni-Co-P/S@C@G	3M KOH	33.16	800	61.5%	[4]

4	$NiCo_2O_4$CNT@DNA	3M KOH	69.7	373.9	96.2/5000	[5]
5	C/$CoNi_3O_4$ NA	3M KOH	19.2	1300	78%/5000	[6]
6	Skutterudite Ni-CoP_3	6M KOH	89.6	796	93%/10000	[7]
7	Ni_xCo_{12-x}Se@NiTe	1M KOH	67.7	724.8	92.4/12000	[8]
8	petal-like Ni–Co–S	1M KOH	79.3	825	91.2% /5000	[9]
9	($Ni_{1.38}Co_{1.62}(PO_4)_2$·8H2O) thin film	1M KOH	42.3	160	83.7/4000	[10]
10	$NiSe_2$-Fe_3Se_4@NiCoB	1M KOH	72.7	710	91.1% /20,000	[11]
11	C-ZIF-800	1 M KOH	141.24	212	100/5000	This work

Reference

1. R. Patil, N. Kumar, S. Bhattacharjee, B. M. Matsagar, P. C. Han, K. C. W. Wu, R. R. Salunkhe, A. Bhaumik and S. Dutta, *Mater. Today Chem.*, 2023, **28**, 101374.
2. X. Zhang, S. Yang, W. Lu, Y. Tian, Z. Liu, Y. Zhao and A. Liu, *Small*, 2022, **18**, 2200656.
3. T. S. Renani, S. M. Khoshfetrat, J. Arjomandi, H. Shi and S. Khazalpour, *J. Mater. Chem. A*, 2021, **9**, 12853-12869.
4. S. Su, L. Sun, J. Qian, X. Shi and Y. Zhang, *ACS Applied Energy Materials*, 2022, **5**, 685-696.
5. Y. Xue, T. Chen, S. Song, P. Kim and J. Bae, *Nano Energy*, 2019, **56**, 751-758.
6. J. Zhu, J. Jiang, Z. Sun, J. Luo, Z. Fan, X. Huang, H. Zhang and T. Yu, *Small*, 2014, **10**, 2937-2945.
7. J. Jiang, Z. Li, X. He, Y. Hu, F. Li, P. Huang and C. Wang, *Small*, 2020, **16**, 2000180.
8. D. Khalafallah, W. Huang, M. Zhi and Z. Hong, *Energy Environ. Mat.*, 2022, **n/a**, e12528.
9. C. Zhang, X. Cai, Y. Qian, H. Jiang, L. Zhou, B. Li, L. Lai, Z. Shen and W. Huang, *Adv. Sci.*, 2018, **5**, 1700375.
10. S. J. Marje, V. V. Patil, V. G. Parale, H.-H. Park, P. A. Shinde, J. L. Gunjakar, C. D. Lokhande and U. M. Patil, *Chem. Eng. J.*, 2022, **429**, 132184.
11. Z. Tian, K. Zhou, M. Xie, Y. Zhang, J. Chen, C. Du and L. Wan, *Chem. Eng. J.*, 2022, **447**, 137495.